Gapped broken symmetry states in ABC-stacked trilayer graphene

Jeil Jung* and Allan H. MacDonald
Department of Physics, University of Texas at Austin, Austin, Texas 78712, USA
(Received 26 July 2012; revised manuscript received 21 April 2013; published 8 August 2013)

We use a self-consistent Hartree-Fock approximation with realistic Coulomb interactions for π-band electrons to explore the possibility of broken symmetry states in weakly disordered ABC-stacked trilayer graphene. The competition between gapped and gapless broken symmetry states and normal states is studied by comparing total energies. We find that gapped states are favored and that, unlike the bilayer case, gapless nematic broken symmetry states are not metastable. Among the gapped states, the layer antiferromagnetic state is favored over anomalous and spin Hall states.

DOI: 10.1103/PhysRevB.88.075408 PACS number(s): 73.22.Pr, 71.15.Nc, 71.70.Gm, 73.22.Gk

I. INTRODUCTION

The electronic structure of few-layer graphene[1,2] systems consists of pairs of bands that cross, or narrowly avoid crossing, near the Fermi level. Because the number of band pairs depends in an interesting way on the stacking arrangement, and because both semimetallic and semiconducting behaviors occur, this family of two-dimensional materials provides an attractive playground for the study of electron interaction effects in systems[3,4] with approximate Fermi points. For example, interactions lead to a marginal Fermi liquid behavior in neutral single-layer graphene,[5,6] and to broken-symmetry ordered states in bilayers.[7–15]

The recent surge of interest in ABC-stacked trilayer graphene[16–28] has motivated theoretical studies of the electron-interaction-induced instabilities that are expected when these structures are weakly disordered. Instabilities are favored in ABC trilayers by extremely flat crossing[2] of a single pair of bands at the neutral system Fermi level, and by exchange energy frustration associated with momentum-space textures in the valence-band wave functions.[29] In the trilayer case, the competition between competing broken symmetry states is massaged by weak remote neighbor hopping processes that reshape the bands at energies within ~20 meV of the crossing point.[30] This energy scale should be compared to the ~ 1 meV scale of analogous processes in bilayer graphene.[31] The remote hopping processes are therefore more likely to play a prominent role in determining how the system responds to electron-electron interactions in the trilayer case.

The broken symmetry states that have been discussed in the bilayer graphene literature can be broadly classified either as gapped phases with broken layer inversion symmetry[7–10] or as gapless nematic states that lower rotational symmetry.[11] Although the two types of states in principle should have clear experimental signatures, it has not yet been possible[13–15] to achieve a universally accepted consensus on the character of the ground state because of the complicated role of residual disorder. Studies of ABC-stacked trilayer graphene could prove to be more unambiguous because its bands are flatter and interaction effects correspondingly stronger, while disorder strengths should be comparable.

In this paper, we present a study of the competition between gapful and gapless states in ABC-stacked trilayer graphene, including the effects of weak remote-hopping processes which can dominate band dispersion very close to the band-crossing (Dirac) point. Interaction physics in this system has also been studied recently under different types of approaches.[32–34] Our study is based on a six-band π-orbital tight-binding model, combined with long-range Coulomb interactions treated using a Hartree-Fock mean-field theory. The quasiparticle band structures of both gapped and gapless states are reshaped when interactions are included. We find that gapped phases are favored over a wide range of the hopping-parameter model space. In mean-field theory, the energy difference between gapped and gapless states is typically smaller than $\sim 10^{-7}$ eV per carbon atom. The small condensation energy reflects the fact that only single-electron states close to the band-crossing points participate in ordering. The strength of the direct hopping process between low-energy sites on the outer layers of the trilayer, γ_2, plays an especially important role in determining the character of the ground state.

II. MODEL HAMILTONIAN

We describe ABC trilayer graphene using a lattice model Hamiltonian with one atomic $2p_z$ orbital per carbon site. We label the six sublattice sites illustrated in Fig. 1(a) as A, B, A', B', A'', B''; the A and B'' sites avoid near-neighbor interlayer coupling, and for this reason they are *low-energy sites* which are dominantly occupied by electrons close to the band-crossing points. With this convention, the six-band tight-binding model Hamiltonian of ABC trilayer graphene is

$$H_0 = -\begin{pmatrix} 0 & \gamma_0 f & 0 & \gamma_3 f^* + \gamma_N & 0 & \gamma_2 \\ \gamma_0 f^* & 0 & \gamma_1 & & 0 & 0 \\ 0 & \gamma_1 & 0 & \gamma_0 f & 0 & \gamma_3 f^* \\ \gamma_3 f + \gamma_N^* & 0 & \gamma_0 f^* & 0 & \gamma_1 & 0 \\ 0 & 0 & 0 & \gamma_1 & 0 & \gamma_0 f \\ \gamma_2 & 0 & \gamma_3 f & 0 & \gamma_0 f^* & 0 \end{pmatrix}, \tag{1}$$

where

$$f(\mathbf{k}) = e^{ik_y a/\sqrt{3}}\left[1 + 2e^{-i3k_y a/2\sqrt{3}} \cos\left(\frac{k_x a}{2}\right)\right] \tag{2}$$

with $a = 2.46$ Å using the same triangular lattice vector convention as in Refs. 4 and 8. The global minus sign in front of the Hamiltonian means that π-bonding bands have lower energy than antibonding bands when the γ parameters

 ©2013 American Physical Society

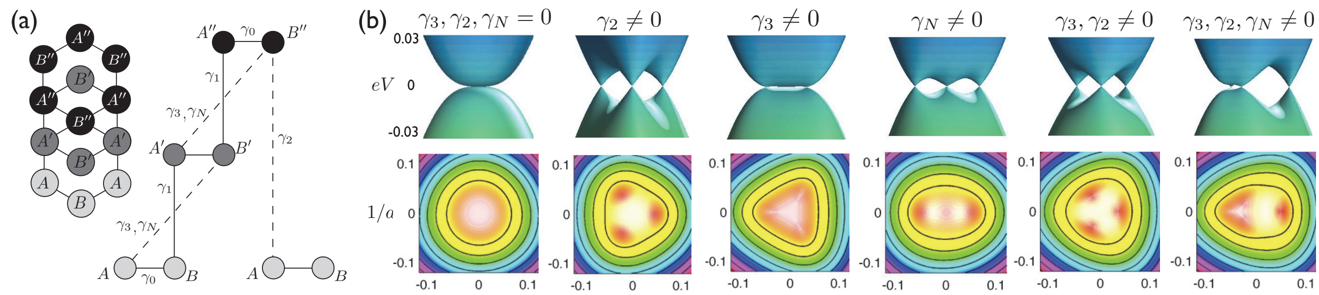

FIG. 1. (Color online) Trilayer graphene unit cell and π-band structure. (a) Schematic representation of the hopping processes included in our model. (b) Band structure near the Dirac point $K=(4\pi/3a,0)$ for different values of the remote hopping parameters. The upper row shows 2D band structures seen from a view rotated by 30° with respect to vertical while the lower row shows the same information expressed in terms of contour plots. When nonzero, the hopping parameters have the values $\gamma_2=0.01$ eV and $\gamma_3=0.3$ eV. We have set $\gamma_4=\gamma_5=0$ throughout our calculations. Wave vectors k are in units of a^{-1}. The γ_2 term splits the Brillouin-zone corner cubic band crossing into three Dirac cones (linear band crossings) located at the vertices of an equilateral triangle. The trigonal γ_3 term acting on its own results in four band-crossing points, including one at the Brillouin-zone corner. When both terms are present simultaneously, the gapless point at K disappears. When the signs of both terms are the same, they tend to produce opposing triangular distortions, whereas if they have opposite signs their triangular distortions are reinforcing. The orientation of the triangular distortion for each of the above parameters is sign-dependent. In realistic band structures, the γ_2 term dominates over γ_3 resulting in three Fermi points with linear dispersion. The nematic term γ_N captures the influence of a layer relative–sliding sliding strain and breaks the triangular rotational symmetry of the bands. We used the value $\gamma_N^0=0.02$ eV in the above illustration.

are positive. In most of our calculations, we have used graphite hopping parameter values that are similar to those in Ref. 35: $\gamma_0=3.12$ eV, $\gamma_1=0.377$ eV, $\gamma_2=0.01$ eV, and $\gamma_3=0.3$ eV. We specifically address the importance of the signs of the remote γ_2 and γ_3 hopping parameters. The near-neighbor intralayer and interlayer hopping processes γ_0 and γ_1 are responsible for broad features of the band structure, while the γ_2 and γ_3 parameters have their main impact close to the band-crossing points. This model qualitatively reproduces the *ab initio* band structure in Ref. 36, in particular capturing the orientation of the triangle formed by the three band-crossing points close to the Brillouin-zone corner. We have ignored the ABC trilayer γ_4 and γ_5 processes that break particle-hole symmetry, and other small on-site terms that are often introduced in models of graphite, because they do not visibly alter the low-energy features of the bands in ABC trilayer graphene.

Using a model similar to that used previously for bilayer graphene,[37,38] we have also examined the influence of a term in the Hamiltonian that is intended to capture the influence on low-energy states of an interlayer relative-translation strain. We write $\gamma_N=\gamma_N^0\exp(-|\mathbf{k}-\mathbf{K}^{(\prime)}|/k_r)$, introducing a damping factor that makes the term small away from the Brillouin-zone corners, where this form for the strain Hamiltonian becomes inaccurate, by setting $k_r=\gamma_1/\hbar\upsilon_F=0.0573$ Å^{-1}.

Because there is some confusion in the literature on the signs of the remote hopping processes, we have also considered other sign choices for γ_2 and γ_3. As shown in Fig. 1(b), direct hopping γ_2 between the low-energy sites A, B''' gives rise to three Fermi points at the vertices of a triangle centered on the Brillouin-zone corner. The trigonal warping (γ_3) process which connects the A,B' and A',B'' sites is also responsible for a trigonal distortion that leads to four Fermi points near K, as in bilayer graphene. Each one of the three Fermi points contributes to a phase winding of 2π for a total 6π phase winding along paths that encircle all three points, as expected in ABC trilayer graphene.[2] (We use the term Fermi point to refer to a band crossing that is tied to the Fermi level of a neutral ABC trilayer. The band-crossing points are exactly at the Fermi level because we have neglected particle-hole symmetry-breaking terms in the band-structure model.) Both γ_2 and γ_3 terms break circular symmetry near the Dirac point by splitting a single Fermi point with cubic band dispersion into multiple Fermi points with linear dispersion. The orientations of the triangular distortion due to γ_2 and γ_3 are opposite when both hopping parameters have the same sign. First-principles band-structure calculations suggest that γ_2 dominates over γ_3 and determines the shape of the bands near the Dirac point. (Note that γ_2 has a much greater influence on the two low-energy states than γ_3 for a given numerical value because it couples them directly, whereas γ_3 acts virtually via high-energy states.) When both terms are present simultaneously and have the same sign, the band structure can have a hybrid shape; for some parameters values, the bands consist of two intertwined triangles with opposite orientations that can exhibit up to nine Dirac cones. The additional parameter, γ_N, couples A,B' and A',B'', like the γ_3 term, but without an accompanying factor $f(\mathbf{k})$. The γ_N term qualitatively describes a band deformation that lowers the crystal rotational symmetry, and is similar to the model used to mimic a small layer-sliding structural deformation in bilayer graphene.[38] This term is also useful to seed lowered rotational symmetry gapless states in our Hartree-Fock calculations.

Electron-electron interaction effects are treated in an unrestricted Hartree-Fock approximation,[4,8] which allows symmetries to be broken:

$$V_{\mathrm{HF}}=\sum_{\mathbf{k}\lambda\lambda'}U_H^{\lambda\lambda'}\left[\sum_{\mathbf{k}'}\langle c^{\dagger}_{\mathbf{k}'\lambda'}c_{\mathbf{k}'\lambda'}\rangle\right]c^{\dagger}_{\mathbf{k}\lambda}c_{\mathbf{k}\lambda}-\sum_{\mathbf{k}'\lambda\lambda'}U_X^{\lambda\lambda'}(\mathbf{k}'-\mathbf{k})\langle c^{\dagger}_{\mathbf{k}'\lambda'}c_{\mathbf{k}'\lambda}\rangle c^{\dagger}_{\mathbf{k}\lambda}c_{\mathbf{k}\lambda'},\qquad(3)$$

where $c^\dagger_{\mathbf{k}\lambda}, c_{\mathbf{k}\lambda}$ are Bloch state creation and annihilation operators, and $\lambda = (l,\sigma)$ lumps lattice and spin indices. The Hartree and exchange Coulomb integrals in Eq. (3),

$$U_H^{ll'} = \frac{1}{A}\sum_{\mathbf{G}} e^{i\mathbf{G}\cdot(\mathbf{s}_l - \mathbf{s}_{l'})} |\widetilde{f}(|\mathbf{G}|)|^2 \ \widetilde{V}^{ll'}(|\mathbf{G}|), \tag{4}$$

$$U_X^{ll'}(\mathbf{q}) = \frac{1}{A}\sum_{\mathbf{G}} \ e^{i\mathbf{G}\cdot(\mathbf{s}_l - \mathbf{s}_{l'})} |\widetilde{f}(|\mathbf{q}-\mathbf{G}|)|^2 \ \widetilde{V}^{ll'}(|\mathbf{q}-\mathbf{G}|), \tag{5}$$

involve sums over reciprocal-lattice vectors $\mathbf{G}$. In these equations, $\mathbf{s}_l$ is the (2D projection of the) position of the sublattice in the unit cell. We used an isotropic atomic orbital form factor $\widetilde{f}(\mathbf{q}) = \int d\mathbf{r}\, e^{-\mathbf{q}\cdot\mathbf{r}}|\phi(\mathbf{r})|^2 = [1-(r_o q)^2]/\{[1+(r_o q)^2]^4\}$ with an artificially large atomic radius $r_o = 3a_o/\sqrt{30}$ to account for sp_2 orbital polarization.[4] Here $a_o = a/(2\sqrt{3})$ is the covalent bond radius of carbon. The two-dimensional Coulomb interactions in Eqs. (4) and (5) are defined by $\widetilde{V}^{ll'}(\mathbf{q}) = 2\pi e^2/(|\mathbf{q}|\epsilon_r)$ when the sublattice indices l and l' refer to the atoms in the same layer, and $[2\pi e^2/(|\mathbf{q}|\epsilon_r)]\exp[-|\mathbf{q}|d]$ when they refer to atoms in layers separated by a distance d.

We used an effective dielectric constant $\varepsilon_r = 4$ in our calculations, partly to account for dielectric screening by surrounding material and partly to account for the well-known tendency of the Hartree-Fock approximation, which neglects screening, to overestimate exchange interaction effects.[39] The present implementation of the lattice model Hartree-Fock mean-field theory follows closely the method described in Refs. 4 and 8 for single and bilayer graphene, which also used a momentum space representation of the Coulomb interaction. One difference in the present implementation is that we sample the full Brillouin zone without taking advantage of the symmetry of the crystal in order to allow for the possibility of broken rotational symmetry nematic phases. Because of the greater importance of states near the Dirac point, we have sampled momentum space nonuniformly; for k points closer than $\sim 0.5/a$ to the Dirac point (where $a = 2.46$ Å is the triangular lattice constant of graphene), we have used a sampling density corresponding to 2304×2304 points in the entire Brillouin zone. Outside this region, we used a matched but coarser sampling with density corresponding to 18×18 points in the Brillouin zone. For a given sampling density, the Hartree-Fock equations are solved iteratively and converged to $\sim 10^{-11}$ eV per carbon atom in total energy.

III. GAPPED AND GAPLESS STATES

As in the AB bilayer case, the low-energy valence-band states of ABC graphene are given approximately by equal-weight coherent sums of top- and bottom-layer wave functions with momentum-dependent phase differences. The gapped broken symmetry states spontaneously increase weight in one of the two layers, whereas[29] the nematic states break the lattice rotational symmetry of the interlayer phases. In the following, we present the results of our π-band Coulomb-interaction Hartree-Fock study. Note that our implementation of the interaction that retains the $1/r$ Coulomb tail offers a more realistic description of electron interactions that improves upon the common short-range Hubbard U approximations, which completely overlook the nonlocal correlations of the electron interaction or truncate its effects of a few nearest neighbors. This mean-field-theory calculation we perform cannot be fully quantitative because it accounts for screening in an ad hoc way, which might be quantitatively inaccurate, and because it neglects higher-order correlation effects. We believe, however, that our results provide some insight into the competition between different potential ordered states, and in particular into the way this competition is influenced by band-structure features particular to ABC trilayer graphene. We first discuss the gapped states, which have spontaneous layer polarizations with spin- or valley-dependent signs, and then ungapped states with lowered rotational symmetry.

A. Condensation energy of gapped phases with spontaneous Hall conductivity

The ABC-stacked multilayer graphene constitutes a physical realization of a chiral 2DEG that, in the presence of an inversion symmetry-breaking *mass* or gap term, develops a valley Hall effect proportional to its layer number[8,9,40,41] approximately proportional to $\sigma_H \sim e^2/h$.[42] Although this approximation, which is valid in the small mass limit, can deviate substantially for large masses,[43] it leads to 1D edge modes and zero-line modes or kink states at interface regions of opposite valley resolved Hall conductivity that can close the gap irrespective of the crystallographic orientation.[40]

In a continuum model, this Hall conductivity remains quantized in fractions of $1/2$ of conductance unit per layer number, valley, and spin.[8,9] In the presence of electron interactions that can introduce a mass term, the energy of the gapped states is minimized when half of the spin-valley components are polarized toward one layer and half toward the other.[8,9] We consider only states of this type, which are favored over other closely related states by electrostatic interactions without a net charge imbalance between one layer to the other. Self-consistent studies in bilayer graphene have shown that peculiar Hall states might be induced when an external inversion symmetry-breaking electric field reduces the electrostatic energy penalty of such charge unbalanced configurations.[8] In a lattice model, there is a clear distinction and an energy difference between states with opposite layer polarizations for different valleys, which have either an anomalous Hall (AH) effect or a spin Hall (SH) effect, and states with opposite layer polarization for opposite spins (LAF), which form an antiferromagnetic state. The three types of ABC trilayer gapped states that have no overall layer polarization are compared in Table I. In our mean-field calculations, anomalous Hall and spin Hall states have the same energy.

We define the condensation energy of the LAF and AH/SH gapped states as their energy relative to the ground-state energy of the unbroken symmetry states. The unbroken symmetry state energy is determined by carrying out self-consistent mean-field calculations that are seeded by the noninteracting electron ground state. We find that the condensation energies for the ordered states are $\sim 10^{-7}$ eV per carbon atom. The condensation energy is approximately three times smaller than the product of the energy gap Δ_{gap} and the charge transferred between layers within individual spins and valleys Δn_l.

The condensation energy scales are approximately five times larger than those obtained for bilayer graphene[8] with

TABLE I. Upper panel: Mean-field theory properties of the three balanced-charge-density gapped states. Each of these states has two of the four valley or spin flavors polarized toward the top layer and two toward the bottom layer; see Ref. 9. Each polarized flavor contributes three quantized e^2/h units to the Hall conductivity with a sign that depends on both valley and layer polarization; the continuum model assignments can be retained in a lattice model because the momentum space Berry curvatures are strongly localized near the Brillouin-zone corners. Middle panel: The density transfer from one outer layer to the other Δn_l for each valley-spin degree of freedom in units of 10^{11} cm^{-2}. (This density scale corresponds to $\sim 1.3 \times 10^{-5}$ electrons per carbon atom.) The total amount of charge transferred per valley or spin is larger in the more stable LAF configuration than the AH or SH configurations. Δ_{gap} is the energy gap in meV. The condensation energies $\Delta E_{\text{cond}} = E_{\text{gapped}} - E_{\text{gapless}}$ shown are differences between the ordered gapped and gapless normal phases in units of 10^{-7} eV per carbon atom. The gapless normal state energies have been obtained from a self-consistent calculation starting from the band orbital seed. The anomalous Hall and spin Hall states have the same energy in mean-field theory. Lower panel: Differences in total energy between LAF and AH/SH states, $\Delta E = E^{\text{LAF}} - E^{\text{AH/SH}}$, in units of 10^{-9} eV per carbon atom. The exchange energy difference per spin or valley is separated into an intravalley (ΔE_X^{KK}) and an intervalley ($\Delta E_X^{KK'}$) contribution. Note that the total exchange energy difference satisfies $\Delta E_X = 4(\Delta E_X^{KK} + \Delta E_X^{KK'})$. Intervalley exchange, normally neglected in continuum models, makes a substantial contribution to the energy difference between LAF and anomalous Hall states.

AF		(λ_z τ_z σ_z)			$\sigma_{xy}^{K,\uparrow}$	$\sigma_{xy}^{K',\uparrow}$	$\sigma_{xy}^{K,\downarrow}$	$\sigma_{xy}^{K',\downarrow}$
AH	$(T\ K\ \uparrow)$	$(B\ K'\ \uparrow)$	$(T\ K\ \downarrow)$	$(B\ K'\ \downarrow)$	3	3	3	3
SH	$(T\ K\ \uparrow)$	$(B\ K'\ \uparrow)$	$(T\ K'\ \downarrow)$	$(B\ K\ \downarrow)$	3	3	−3	−3
LAF	$(T\ K\ \uparrow)$	$(T\ K'\ \uparrow)$	$(B\ K\ \downarrow)$	$(B\ K'\ \downarrow)$	3	−3	−3	3
	Δn_l^{LAF}	Δn_l^{AH}	$\Delta_{\text{gap}}^{\text{LAF}}$	$\Delta_{\text{gap}}^{\text{AH}}$	$\Delta E_{\text{cond}}^{\text{LAF}}$	$\Delta E_{\text{cond}}^{\text{AH}}$		
$\gamma_2,\gamma_3 = 0$	1.22	1.21	65.1	64.9	−3.599	−3.554		
$\gamma_2,\gamma_3 > 0$	1.09	1.08	56.0	55.6	−1.716	−1.680		
$\gamma_2 < 0,\gamma_3 > 0$	0.12	0.10	12.1	11.7	0.00039	0.00046		
	ΔE_{tot}	ΔE_X	ΔE_X^{KK}	$\Delta E_X^{KK'}$				
$\gamma_2,\gamma_3 = 0$	−4.43	−14.02	−2.62	−0.88				
$\gamma_2,\gamma_3 > 0$	−3.58	−13.81	−2.77	−0.68				
$\gamma_2 < 0,\gamma_3 > 0$	−0.0065	−1.660	−0.4154	0.0005				

similar approximations, presumably because the crossing bands are even flatter in the trilayer case, thus they have a higher density of states and the role of interactions is enhanced. The band gaps we calculate and present in Table I are roughly ten times larger than the spontaneous gap values $\sim$6 meV estimated from transport measurements in ABC trilayer graphene,[16] and between 1.6 and 2 times larger than the gaps ($\sim$30 meV) obtained for the bilayer graphene using the same value of $\varepsilon_r = 4$.[8] This could suggest that screening effects are underestimated by this value of ε_r, or that other interaction effects that are absent in mean-field theories play an essential role. In first-principles calculations, the damping of the strength of exchange, say by a factor of $\sim$2, is common practice[39] to account for Coulomb correlation screening missing in an exchange-only theory. This type of consideration motivates our choice for the dielectric constant, which is larger than what would be suggested by dielectric screening considerations alone, adding some uncertainty to any quantitative predictions. Experimentally the ratio of trilayer to bilayer gaps is $\sim$2.5, close to the ratio we obtain. This suggests that the choice $\varepsilon_r = 4$ quantitatively overestimates exchange effects in both cases. The discrepancy between theory and experiment could, however, be due in part to the unfavorable influence of disorder in experimental samples, and also in part to inaccuracies in our band-structure model, which relies on hopping parameters obtained from graphite. The presence of disorder leads to impurity states within the gap that will enhance the screening of electron interaction, which in turn can lead to a suppression of the interaction-driven spontaneous gap. Further experiments on trilayer graphene with improved quality with controlled disorder levels comparable with those of bilayer or single-layer samples would help to shed light on our discussions.

B. Parameter sweep and band reshaping due to distant hopping terms

The band Hamiltonian introduced and discussed in Sec. II include hopping terms beyond the minimal model to capture the band reshaping that is expected to take place in the ABC trilayer. In the calculation results of Table I, we can observe, for example, that the gapped states are strongly suppressed when γ_2 and γ_3 have opposite signs, separating the Fermi points of the three Dirac cones. On the other hand, when γ_2 and γ_3 have the same sign, the overall effect is that of restoring the approximate circular symmetry of the bands, enhancing the chances for a gapped phase.

Our calculations find that the nematic broken symmetry state is not stable in ABC trilayers. When we iterate the Hartree-Fock equations starting from a nematic seed, lattice rotational symmetry is restored at convergence. In both $\gamma_2 = \gamma_3 = 0$ and the more realistic $\gamma_2,\gamma_3 \neq 0$ case, the same unbroken symmetry state with three band-crossing points is reached for self-consistent calculations starting from either nematic or band seeds. This result is different from the one obtained in the graphene bilayer case, in which the same type of calculation yields a stable gapless state which lowers the crystal's rotational symmetry, giving rise to a nematic order.[44]

The gapped solution of the Hartree-Fock equations lowers the total energy of the system by avoiding rapid in-plane xy rotation of the sublattice pseudospin direction near the band-crossing point.[7] The gapless nematic phase lowers the total energy of the system by reducing the wave-vector dependence of intersite phase differences and introduces an anisotropic renormalization of the band velocity. The competition between the two broken symmetry phases depends on how much energy can be gained by reshaping the quasiparticle bands in two

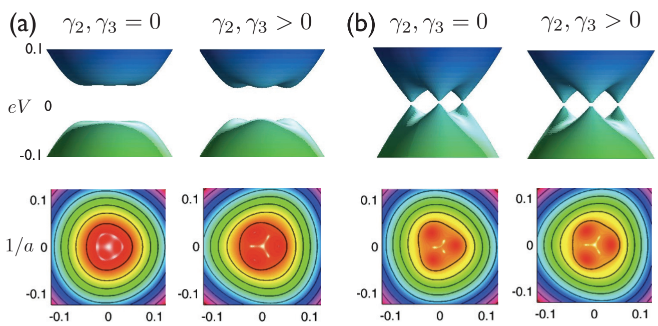

FIG. 2. (Color online) Self-consistent Hartree-Fock calculations iterated from seeds for the gapped and gapless nematic states in ABC trilayer graphene. The gapped solution (a) has been obtained starting from the layer antiferromagnetic initial condition, while the gapless self-consistent solution (b) has been obtained by seeding with a nematic γ_N term. Note that the gapless solutions restore the rotational symmetry of the crystal lattice that was broken by the γ_N term, indicating that nematic order is not stable at the mean-field level in the trilayer case. When the remote hopping parameters $\gamma_2 = 0.01$ eV and $\gamma_3 = 0.3$ eV are accounted for, they induce a triangular distortion of the bands near the Dirac point and determine the angles at which the band crossings occur.

different ways. Figure 2 shows the band structures obtained from self-consistent calculations with gapped and nematic seeds. The remote hopping terms introduce a triangular distortion in the shape of the bands near the Fermi energy, but they do not greatly influence the gapped state properties. These distortions will have important consequences for the electronic properties of doped ABC trilayers. It is noteworthy that the gapless phase within the minimal model develops a three-Fermi-point structure due to electron interactions alone, although it does not lower the rotational symmetry of the crystal. In the picture of an effective two-dimensional low-energy model, this would be an additional off-diagonal term introduced by the electron interaction that does not break any symmetry but enhances the triangular distribution features of the Dirac cones dictated by the band term. Hence, the presence of the γ_2, γ_3 terms also plays a role in determining the orientation of the triangular deformation the bands undergo near the Dirac points in the gapless state. Although we have found that the gapless phases are not the preferred ground state from a total energy for a wide range of hopping parameter values, they might be favored in certain conditions of straining and disorder or disorder that screens out the gapped phase. In such cases, the signatures of electronic interaction can be manifested through an enhancement of the triangular Dirac cones distribution.

Motivated by uncertainty in the values of the remote hopping process parameters, we have performed self-consistent calculations over a range of values of the γ_2, γ_3, and γ_N parameters. The dependence of the energy difference between the interaction-driven gapped and gapless states on model parameters is summarized in Fig. 3. We find that the gapped phase almost always has a lower total energy than the gapless phase. However, as expected, when the remote hopping processes are stronger, the difference in the total energy between the gapped and gapless phases becomes smaller. Figure 3 shows that the occurrence of the gapped phase relies on the principal intralayer and interlayer processes, whose strength is defined by γ_0 and γ_1, and by the flatness of the crossing between conduction and valence bands that their dominance implies.

IV. DISCUSSION

We have used a Hartree-Fock mean-field-theory calculation to demonstrate that electron interactions can lead to ordered phases in ABC trilayer graphene, provided that the strengths of the remote hopping process in this two-dimensional crystal are close to current estimates. In ABC trilayers, bands near the Dirac point are strongly influenced by the γ_2 parameter over

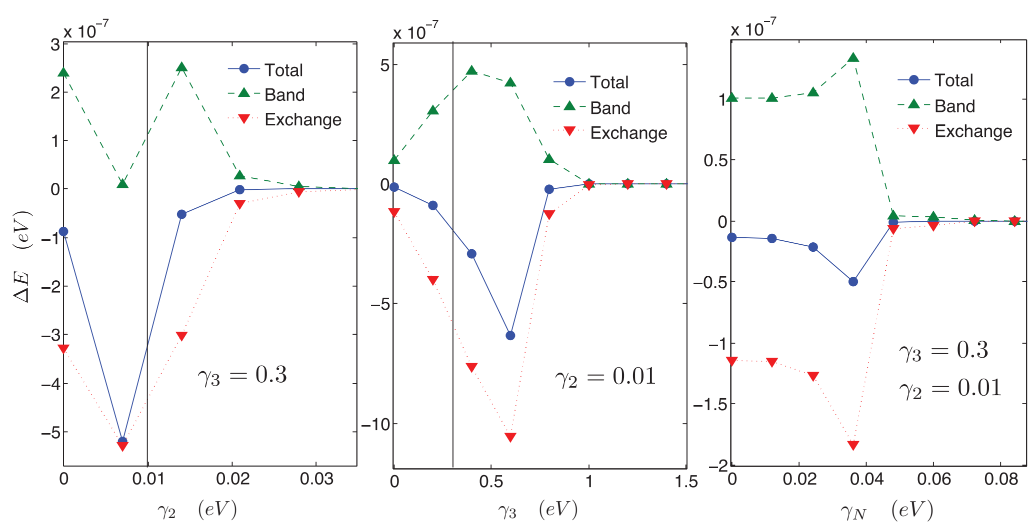

FIG. 3. (Color online) Energy difference between gapped and gapless states $\Delta E = E_{\text{gapped}} - E_{\text{gapless}}$ as a function of γ_2, γ_3, and γ_N. For $\gamma_N = 0$, the lattice symmetry of the gapless state is not lowered by interactions. The vertical black solid lines indicate the hopping parameters $\gamma_2 = 0.01$ eV and $\gamma_3 = 0.3$ eV that best approximate the band structure predicted by *ab initio* DFT calculations. For strong remote hopping processes, the gap in the gapped state closes progressively and the energy difference between gapped and ungapped states is reduced progressively.

energy scales of ∼20 meV, compared to the ∼1 meV scale over which analogous processes play a role in AB bilayers. The physics of their interplay with interactions is therefore less likely to be distorted by disorder. Remote hopping processes in ABC trilayers can be important in fixing the shape of the energy bands near the Fermi level. We have shown that the gapped broken symmetry phases are nevertheless preferred energetically over gapless states for a wide range of remote hopping parameters. We find that our gapless solutions do not lower the crystal symmetry, although they do generally lead to the formation of a triple Dirac point at the vertices of an equilateral triangle. The nematic phase that would break the triangular crystal symmetry is not stable. When remote hopping processes are included, the location of the Dirac points is fixed by the γ_2 process.

There are three distinct gapped states which have very similar energies. Among these, the anomalous Hall and spin Hall (AH and SH) states have the same energy within mean-field theory, whereas the layer antiferromagnet state is distinct and is favored by intervalley exchange because electrons with the same spin state have the same sense of layer polarization. We find that the difference in total energy between LAF and AH/SH is two orders of magnitude smaller than the condensation energy of either state. In our view, these states should therefore be considered as close cousins. Real samples are likely to be found in configurations in which several phases are present separated by domain walls. An external magnetic field which favors anomalous Hall states, at least at finite carrier densities, could be used as a knob to manipulate the domain structure.

Using the Hartree-Fock approximation and reducing interaction strengths by a factor of $\varepsilon_r = 4$, we find that ABC trilayer graphene has a substantial interaction driven gap of the order of 65 meV. The size of the gap is sensitive to the choice we have made for the ε_r parameter, which we have chosen to mimic exchange interaction renormalization parameters that are used in *ab initio* hybrid-density-functional calculations. Band-structure effects can reduce the size of the gap substantially when γ_2 and γ_3 are assigned with values of opposite sign. For favorable parameters, the gaps we find are approximately twice as large as those predicted values for bilayer graphene using corresponding approximations. The theoretical gaps for the minimal model are therefore very much larger than initial estimates of a spontaneous band gap from ABC trilayer experiments, which suggest a value ∼6 meV.[16] The discrepancy is certainly due in part to disorder and inhomogeneity, which reduces the gaps of experimental systems below ideal values but could also reflect a theoretical overestimate. We note in this connection that ABC trilayer graphene samples generally have poorer quality than bilayers. This difference could be due to the lower effectiveness of the current annealing procedure routinely applied to suspended graphene single or multilayer samples. Future experimental work may establish a higher lower bound for the trilayer graphene gap.

Note added: Our recent electronic structure calculations for trilayer graphene based on Wannier localized functions indicate that γ_2 and γ_3 effective hopping parameters have opposite signs, which corresponds to the less favorable parameter set for the gapped phase.

ACKNOWLEDGMENTS

This work was supported by SWAN, by Welch Foundation Grant No. TBF1473, and by DOE Division of Materials Sciences and Engineering Grant No. DE-FG03-02ER45958. We gratefully acknowledge assistance and computer hours from the Texas Advanced Computing Center.

*jeil@physics.utexas.edu

[1] F. Guinea, A. H. Castro Neto, and N. M. R. Peres, Phys. Rev. B **73**, 245426 (2006); H. Min and A. H. MacDonald, *ibid.* **77**, 155416 (2008).

[2] H. Min and A. H. MacDonald, Prog. Theor. Phys. Suppl. **176**, 227 (2008).

[3] A. A. Abrikosov and S. D. Beneslavskii, Zh. Eksp. Teor. Fiz. **59**, 1280 (1970) [Sov. Phys. JETP **32**, 699 (1971)].

[4] J. Jung and A. H. MacDonald, Phys. Rev. B **84**, 085446 (2011).

[5] J. Gonzalez, F. Guinea, and M. A. H. Vozmediano, Phys. Rev. B **59**, R2474 (1999); Phys. Rev. Lett. **77**, 3589 (1996); Nucl. Phys. B **424**, 595 (1994).

[6] D. C. Elias, R. V. Gorbachev, A. S. Mayorov, S. V. Morozov, A. A. Zhukov, P. Blake, L. A. Ponomarenko, I. V. Grigorieva, K. S. Novoselov, F. Guinea, and A. K. Geim, Nat. Phys. **7**, 701 (2011), and work cited therein.

[7] H. Min, G. Borghi, M. Polini, and A. H. MacDonald, Phys. Rev. B **77**, 041407(R) (2008).

[8] J. Jung, F. Zhang, and A. H. MacDonald, Phys. Rev. B **83**, 115408 (2011).

[9] F. Zhang, J. Jung, G. A. Fiete, Q. Niu, and A. H. MacDonald, Phys. Rev. Lett. **106**, 156801 (2011).

[10] F. Zhang, H. Min, M. Polini, and A. H. MacDonald, Phys. Rev. B **81**, 041402(R) (2010); R. Nandkishore and L. Levitov, Phys. Rev. Lett. **104**, 156803 (2010); Phys. Rev. B **82**, 115124 (2010); **82**, 115431 (2010); T. C. Lang, Z. Y. Meng, M. M. Scherer, S. Uebelacker, F. F. Assaad, A. Muramatsu, C. Honerkamp, and S. Wessel, Phys. Rev. Lett. **109**, 126402 (2012); F. Freitag, M. Weiss, R. Maurand, J. Trbovic, and C. Schönenberger, Solid State Commun. **152**, 2053 (2012); F. Zhang, H. Min, and A. H. MacDonald, Phys. Rev. B **86**, 155128 (2012); W. Bao, J. Velasco Jr., F. Zhang, L. Jing, B. Standley, D. Smirnov, M. Bockrath, A. H. MacDonald, and C. N. Lau, Proc. Natl. Acad. Sci. (USA) **109**, 10802 (2012); E. V. Gorbar, V. P. Gusynin, V. A. Miransky, and I. A. Shovkovy, Phys. Rev. B **85**, 235460 (2012); M. Kharitonov, *ibid.* **86**, 195435 (2012); G. M. Rutter, S. Jung, N. N. Klimov, D. B. Newell, N. B. Zhitenev, and J. A. Stroscio, Nat. Phys. **7**, 649 (2011).

[11] O. Vafek and K. Yang, Phys. Rev. B **81**, 041401(R) (2010); O. Vafek, *ibid.* **82**, 205106 (2010); R. E. Throckmorton and O. Vafek, *ibid.* **86**, 115447 (2012); V. Cvetkovic, R. E. Throckmorton, and O. Vafek, *ibid.* **86**, 075467 (2012).
[12] M. M. Scherer, S. Uebelacker, and C. Honerkamp, Phys. Rev. B **85**, 235408 (2012); Y. Lemonik, I. L. Aleiner, C. Toke, and V. I. Falko, *ibid.* **82**, 201408(R) (2010); Y. Lemonik, I. L. Aleiner, and V. I. Fal'ko, *ibid.* **85**, 245451 (2012).
[13] J. Velasco Jr., L. Jing, W. Bao, Y. Lee, P. Kratz, V. Aji, M. Bockrath, C. N. Lau, C. Varma, R. Stillwell, D. Smirnov, F. Zhang, J. Jung, and A. H. MacDonald, Nat. Nanotech. **7**, 156 (2012); F. Freitag, J. Trbovic, M. Weiss, and C. Schonenberger, Phys. Rev. Lett. **108**, 076602 (2012).
[14] A. S. Mayorov, D. C. Elias, M. Mucha-Kruczynski, R. V. Gorbachev, T. Tudorovskiy, A. Zhukov, S. V. Morozov, M. I. Katsnelson, V. I. Fal'ko, A. K. Geim, and K. S. Novoselov, Science **333**, 860 (2011).
[15] B. Feldman, J. Martin, and A. Yacoby, Nat. Phys. **5**, 889 (2009); R. T. Weitz, M. T. Allen, B. E. Feldman, J. Martin, and A. Yacoby, Science **330**, 812 (2010).
[16] W. Bao, L. Jing, Y. Lee, J. Velasco Jr., P. Kratz, D. Tran, B. Standley, M. Aykol, S. B. Cronin, D. Smirnov, M. Koshino, E. McCann, M. Bockrath, and C. N. Lau, Nat. Phys. **7**, 948 (2011).
[17] L. Zhang, Y. Zhang, J. Camacho, M. Khodas, and I. A. Zaliznyak, Nat. Phys. **7**, 953 (2011).
[18] C. H. Lui, Z. Li, K. F. Mak, E. Cappelluti, and T. F. Heinz, Nat. Phys. **7**, 944 (2011).
[19] S. H. Jhang, M. F. Craciun, S. Schmidmeier, S. Tokumitsu, S. Russo, M. Yamamoto, Y. Skourski, J. Wosnitza, S. Tarucha, J. Eroms, and C. Strunk, Phys. Rev. B **84**, 161408(R) (2011).
[20] M. Koshino, Phys. Rev. B **81**, 125304 (2010).
[21] W. Norimatsu and M. Kusunoki, Phys. Rev. B **81**, 161410 (2010).
[22] J. H. Warner, M. Mukai, and Al. Kirkland, ACS Nano. **6**, 5680 (2012).
[23] C. H. Ho, Y. H. Ho, Y. H. Chiu, Y. N. Chen, and M. F. Lin, Ann. Phys. (NY) **326**, 721 (2011).
[24] S. Bala Kumar and J. Guo, Appl. Phys. Lett. **100**, 163102 (2012).
[25] S. Yuan, R. Roldan, and M. I. Katsnelson, Phys. Rev. B **84**, 125455 (2011).
[26] F. Zhang, D. Tilahun, and A. H. MacDonald, Phys. Rev. B **85**, 165139 (2012).
[27] M. Nakamura and L. Hirasawa, Phys. Rev. B **77**, 045429 (2008).
[28] M. Trushin and J. Schliemann, New J. Phys. **14**, 095005 (2012).
[29] A. H. MacDonald, J. Jung, and F. Zhang, Phys. Scr. T **146**, 014012 (2012).
[30] M. Koshino and E. McCann, Phys. Rev. B **80**, 165409 (2009); F. Zhang, B. Sahu, H. Min, and A. H. MacDonald, *ibid.* **82**, 035409 (2010).
[31] E. McCann and V. I. Fal'ko, Phys. Rev. Lett. **96**, 086805 (2006).
[32] D.-H. Xu, J. Yuan, Z.-J. Yao, Y. Zhou, J.-H. Gao, and F.-C. Zhang, Phys. Rev. B **86**, 201404(R) (2012).
[33] M. M. Scherer, S. Uebelacker, D. D. Scherer, and C. Honerkamp, Phys. Rev. B **86**, 155415 (2012).
[34] V. Cvetkovic and O. Vafek, arXiv:1210.4923.
[35] B. Partoens and F. M. Peeters, Phys. Rev. B **74**, 075404 (2006).
[36] S. Latil and L. Henrard, Phys. Rev. Lett. **97**, 036803 (2006).
[37] Y-W. Son, S.-M. Choi, Y. P. Hong, S. Woo, and S. H. Jhi, Phys. Rev. B **84**, 155410 (2011).
[38] M. Mucha-Kruczynski, I. L. Aleiner, and V. I. Fal'ko, Phys. Rev. B **84**, 041404 (2011).
[39] J. C. Slater, Phys. Rev. **81**, 385 (1951); A. Seidl, A. Görling, P. Vogl, J. A. Majewski, and M. Levy, Phys. Rev. B **53**, 3764 (1996).
[40] J. Jung, F. Zhang, Z. H. Qiao, and A. H. MacDonald, Phys. Rev. B **84**, 075418 (2011).
[41] X. Li, Z. H. Qiao, J. Jung, and Q. Niu, Phys. Rev. B **85**, 201404(R) (2012).
[42] D. Xiao, W. Yao, and Q. Niu, Phys. Rev. Lett. **99**, 236809 (2007).
[43] J. Jung, Z. H. Qiao, Q. Niu, and A. H. MacDonald, Nano Lett. **12**, 2936 (2012).
[44] J. Jung *et al.* (unpublished).